Geochemistry Geophysics Geosystems G3
AN ELECTRONIC JOURNAL OF THE EARTH SCIENCES
Published by AGU and the Geochemical Society

Article
Volume 10, Number 12
22 December 2009
Q12011, doi:10.1029/2008GC002353
ISSN: 1525-2027

Salinity bias on the foraminifera Mg/Ca thermometry: Correction procedure and implications for past ocean hydrographic reconstructions

Elise Mathien-Blard and Franck Bassinot
LSCE, CEA, UVSQ, CNRS, Domaine du CNRS, F-91198 Gif-sur-Yvette, France
(franck.bassinot@lsce.cnrs-gif.fr)

[1] Mg/Ca in foraminiferal calcite has recently been extensively used to estimate past oceanic temperatures. Here we show, however, that the Mg/Ca temperature relationship of the planktonic species *Globigerinoides ruber* is significantly affected by seawater salinity, with a +1 psu change in salinity resulting in a +1.6°C bias in Mg/Ca temperature calculations. If not accounted for, such a bias could lead, for instance, to systematic overestimations of Mg/Ca temperatures during glacial periods, when global ocean salinity had significantly increased compared to today. We present here a correction procedure to derive unbiased sea surface temperatures (SST) and $\delta^{18}O_{sw}$ from *G. ruber* $T_{Mg/Ca}$ and $\delta^{18}O_f$ measurements. This correction procedure was applied to a sedimentary record to reconstruct hydrographic changes since the Last Glacial Maximum (LGM) in the Western Pacific Warm Pool. While uncorrected $T_{Mg/Ca}$ data indicate a 3°C warming of the Western Pacific Warm Pool since the LGM, the salinity-corrected SST result in a stronger warming of 4°C.

Components: 10,959 words, 5 figures, 5 tables.

Keywords: Mg/Ca thermometry.

Index Terms: 4954 Paleoceanography: Sea surface temperature; 4924 Paleoceanography: Geochemical tracers; 4926 Paleoceanography: Glacial.

Received 1 December 2008; **Revised** 21 September 2009; **Accepted** 28 September 2009; **Published** 22 December 2009.

Mathien-Blard, E., and F. Bassinot (2009), Salinity bias on the foraminifera Mg/Ca thermometry: Correction procedure and implications for past ocean hydrographic reconstructions, *Geochem. Geophys. Geosyst.*, *10*, Q12011, doi:10.1029/2008GC002353.

1. Introduction

[2] Among the various proxies developed to reconstruct past sea surface temperatures (SST), the Mg/Ca measured on planktonic foraminifera has been given much attention these recent years because it also makes it possible to estimate paleo-seawater $\delta^{18}O$ (related to SSS) by combining $T_{Mg/Ca}$ with stable oxygen isotope measurements ($\delta^{18}O_f$) performed on the same shells [*Mashiotta et al.*, 1999; *Rashid et al.*, 2007; *Levi et al.*, 2007].

[3] The link between calcite Mg/Ca and temperature was first observed from inorganic precipitation experiments, which showed an exponential thermodynamic temperature dependence of calcite Mg/Ca, with Mg/Ca increasing with increasing precipitation temperature [*Oomori et al.*, 1987]. Culture experiments and core top calibrations demonstrated that this relationship to temperature also largely controls the Mg/Ca of foraminiferal calcite [*Elderfield and Ganssen*, 2000; *Lea et al.*, 2000; *Cléroux et al.*,

2008]. However, several potential biases have been identified.

[4] Carbonate dissolution at the seafloor is the best known of those potential biases affecting the Mg/Ca of foraminifera shells. Because Mg-calcite is more soluble than pure calcite, the Mg/Ca of foraminifera calcite diminishes with increasing dissolution owing to the preferential removal of the Mg/Ca-richest areas of the shell [*Brown and Elderfield*, 1996; *Dekens et al.*, 2002; *Beck et al.*, 2002; *Nouet and Bassinot*, 2007]. *Levi* [2003] has shown, for instance, that this dissolution effect results in the apparent decrease of 0.6°C/km of the temperature derived from Mg/Ca estimated from *Globigerinoides ruber* shells picked from surface sediments along a depth transect on the Sierra Leone Rise. Several approaches have been proposed to correct this dissolution effect on Mg/Ca thermometry [*Dekens et al.*, 2002; *Rosenthal and Lohmann*, 2002].

[5] There are other potential biases on Mg/Ca thermometry, which are not clearly understood nor dealt with at present. Culture experiments of *Globigerinoides bulloides* and *Orbulina universa* [*Russell et al.*, 2004] and *G. ruber* [*Kisakürek et al.*, 2008] suggest that Mg/Ca is negatively related to the carbonate ion content of seawater when $[CO_3^{2-}]$ values are below 200 μmol kg^{-1}. These culture studies suggest, however, that planktonic foraminifera Mg/Ca is not affected by carbonate ion concentration at usual, ambient seawater ranges (200 μmol kg^{-1} < $[CO_3^{2-}]$ < 300 μmol kg^{-1}).

[6] Laboratory culture experiments also suggest that there exists a relationship between foraminiferal Mg/Ca and seawater salinity. *Nürnberg et al.* [1996], for instance, showed that a 10 psu change in salinity induces a 110% Mg/Ca increase in cultured *Globigerinoides sacculifer* shells. For *O. universa*, the salinity effect appears to be significantly weaker, with a Mg/Ca increase of only 4 ± 3% per psu change [*Lea et al.*, 1999]. This smaller effect is similar to that observed from culture experiments carried out on *G. ruber* [*Kisakürek et al.*, 2008], which showed a salinity dependency with an exponential Mg/Ca increase of 5 ± 3%/psu.

[7] Recent works performed on core top material seem to confirm that foraminiferal Mg/Ca may be significantly affected by salinity [*Ferguson et al.*, 2008; *Arbuszewski et al.*, 2008]. Based on a core top study in the Mediterranean Sea, *Ferguson et al.* [2008] concluded that in areas of high salinity (>36 psu), significant salinity biases can be expected on the Mg/Ca paleothermometer. However, *Ferguson et al.*'s [2008] Mg/Ca results may be questioned since foraminiferal shells from Mediterranean deep-sea sediments appear to be coated by a postdepositional Mg-rich calcite layer [*Sexton et al.*, 2006]. To this date, therefore, there are only sparse data that document the salinity effect on Mg/Ca thermometer and this effect was usually neglected by authors using foraminiferal Mg/Ca for paleo-SST reconstructions.

[8] In order to test the possible carbonate ion and salinity effects on Mg/Ca thermometry of *G. ruber* (a species frequently used for reconstructing sea surface paleohydrology of low latitudes and mid-latitudes), we studied core top material retrieved above the lysocline (to minimize dissolution effects) from several areas from the North Atlantic, the Red Sea, and the tropical Indian and western Pacific Oceans. These areas cover a wide range of modern sea surface salinities (32 psu < SSS < 37 psu) and $[CO_3^{2-}]$ concentrations (170 < $[CO_3^{2-}]$ < 260 μmol kg^{-1}).

[9] Implications for paleoreconstructions of SST and SSS (obtained by combining *G. ruber* $T_{Mg/Ca}$ and $\delta^{18}O$) will be discussed, and we will propose an approach to minimize systematic biases. The correction procedure will be applied to a sedimentary record from the tropical Indian Ocean to illustrate the implications of salinity bias on Mg/Ca SST and $\delta^{18}O_{sw}$ reconstructions since the Last Glacial Maximum (LGM).

2. Sample Selection and Hydrographic Settings

[10] We obtained marine sediment core tops from high sedimentation rate areas of the North Atlantic, the southeastern Red Sea, the Arabian Sea, the Bay of Bengal, the Indonesian Archipelago region, and the western Pacific Ocean. We estimated, at each site, the bottom water departure from calcite saturation (ΔCO_3^{2-}) based on the gridded bottom water $[CO_3^{2-}]$ atlas from *Archer* [1996] and using the revised empirical equation of $[CO_3^{2-}]$ at saturation ($[CO_3^{2-}]_{sat}$) versus water depth from *Bassinot et al.* [2004]. For our Atlantic Ocean core tops, bottom water ΔCO_3^{2-} is high at all sites, ranging from +26.3 to +93.7 μmol kg^{-1} (Table 1a), which clearly suggests that dissolution at the seafloor is not a major issue. The lack of significant dissolution is confirmed by the very good preservation of the foraminifera shells and the small amount of test fragmentation.

[11] In the Indian and west Pacific Oceans, *Broecker and Clark* [1999] had analyzed surface

Table 1a. Core Top and Locations[a]

Area	Core Top	Latitude	Longitude	Water Depth (m)	Age Control[b]	CO_3^{2-} (μmol kg^{-1})	ΔCO_3^{2-} (μmol kg^{-1})
North Atlantic	INMD48BX.1	29°49′N	43°13′W	2836	3 and 4	106.6	38.2
North Atlantic	INMD68BX.6	34°48′N	28°22′W	2520	3 and 4	107.0	42.3
North Atlantic	MD95-2038	37°45′N	20°11′W	2310	4	110.1	47.7
North Atlantic	paleo SU 9007P	42°30′N	32°21′W	3290	4	108.7	34.8
North Atlantic	paleo SU 9004P	41°00′N	32°00′W	2865	4	95.0	26.3
North Atlantic	paleo SU 9002P	40°34′N	30°57′W	2220	3	110.5	49.1
North Atlantic	paleo SU 9003P	40°03′N	32°00′W	2475	2 and 3	103.7	39.5
North Atlantic	paleo SU 9008P	43°50′N	30°35′W	3080	3 and 4	110.7	39.4
North Atlantic	paleo SU 9006P	42°00′N	32°40′W	3510	3	109.3	32.5
North Atlantic	CHO 288-54	17°26′N	77°39′W	1020	1	97.5	47.6
North Atlantic	MD95-2002	47°27′N	8°32′W	2174	3 and 4	111.4	50.4
North Atlantic	MD99-2203	34°58′N	75°12′W	620	1	140.3	93.7
Mozambic	MD79-255	19°00′S	37°30′E	1226	4	72.3	20.6
Mozambic	MD79-257	20°24′S	36°20′E	1262	2	71.0	18.9
Arabian Sea	MD92-1002	12°01′N	44°19′E	1327	1	61.5	8.9
Indonesia	MD00-2359 PC	9°13′S	114°43′E	2775	4	85.1	17.5
Indonesia	MD 98-2165	9°39′S	118°20′E	2100	1	75.1	14.9
Andaman Sea	MD77-176	14°31′N	93°08′E	1375	1	69.5	16.4
Southeast India	MD00-2360top	20°05′S	112°40′E	980	4	69.8	20.2
Red Sea	MD92-1008	14°26′N	42°14′E	708	1	186.0	138.7
Indonesia	MD002358top	12°17′S	112°43′E	2520	4	95.8	31.1
Indonesia	MD00-2359 G	9°13′S	114°43′E	2775	4	85.1	17.5
Arabian Sea	ODP117-723	18°03′N	57°37′E	808	1	64.9	16.8
Central India	MD77-191	07°30′N	76°43′E	1254	1	59.6	7.6
West Pacific	ERDC92BX	2°14′S	157°00′E	1598	2	63.2	8.0

[a] Cores were collected with a piston corer except samples marked with BX (box core), PC (pilot core), and G (gravity core). Bottom water [CO_3^{2-}] values are taken from *Archer*'s [1996] database, and ΔCO_3^{2-} values are estimated from *Bassinot et al.* [2004].

[b] Chronostratigraphic quality levels (age control) are given from 1 to 4, corresponding to different levels of uncertainty. Numbers 1 and 2 correspond to AMS-^{14}C radiometric control within the intervals 0–2 ka and 0–6 ka, respectively; level 3 is used for specific biostratigraphic control (i.e., % of *Globorotalia hirsuta* left coiling in the North Atlantic); and level 4 indicates other stratigraphic control, such as *G. ruber* δ^{18}O.

sediment dissolution using a quantitative, $CaCO_3$ size dissolution index. They concluded that sediments are not significantly affected by dissolution in core tops with index values greater than 0.56 [*Broecker and Clark*, 1999]. Regression calculations performed on Broecker and Clark's data plotted versus bottom water ΔCO_3^{2-} show that the well-preserved, surface sediments correspond to bottom water ΔCO_3^{2-} which are above ~6 μmol kg^{-1} in the eastern Indian Ocean and western Pacific Ocean, and above ~15 μmol kg^{-1} in the western Indian Ocean. We rejected from our Indo-Pacific database the core tops that show bottom water ΔCO_3^{2-} lower than those threshold values (Table 1a). The fact that these dissolution thresholds correspond to bottom water slightly more supersaturated relative to calcite in the western than in the eastern tropical Indian Ocean could indicate a generally more intense respiration-driven dissolution in sediments from the western Indian Ocean, due to a generally higher primary productivity. The low level of foraminifera fragmentation observed in the core top samples that we kept in our database confirms that they are well preserved. This is also indicated by the presence of pteropods in some samples such as the core top of core MD92-1002, located in the Gulf of Aden.

[12] The final, well-preserved sediment collection used for this study contains 25 core tops from 24 different locations (Figure 1 and Table 1a). Late Holocene ages are verified by radiometric dates, foraminiferal counts or isotopic stratigraphy as defined in MARGO [*Kucera et al.*, 2005]. In addition, we used five plankton tow samples from the western Pacific area, for which in situ surface temperatures were measured during plankton tow operations (Table 1b).

3. Analytical Measurements

[13] Isotopic and trace element analyses were performed on the shallow-dwelling species *G. ruber* (white in a strict sense) [*Wang*, 2000]. *G. ruber* specimens were picked in the narrow 250–315 μm size fraction to minimize possible size effects [*Elderfield et al.*, 2002].

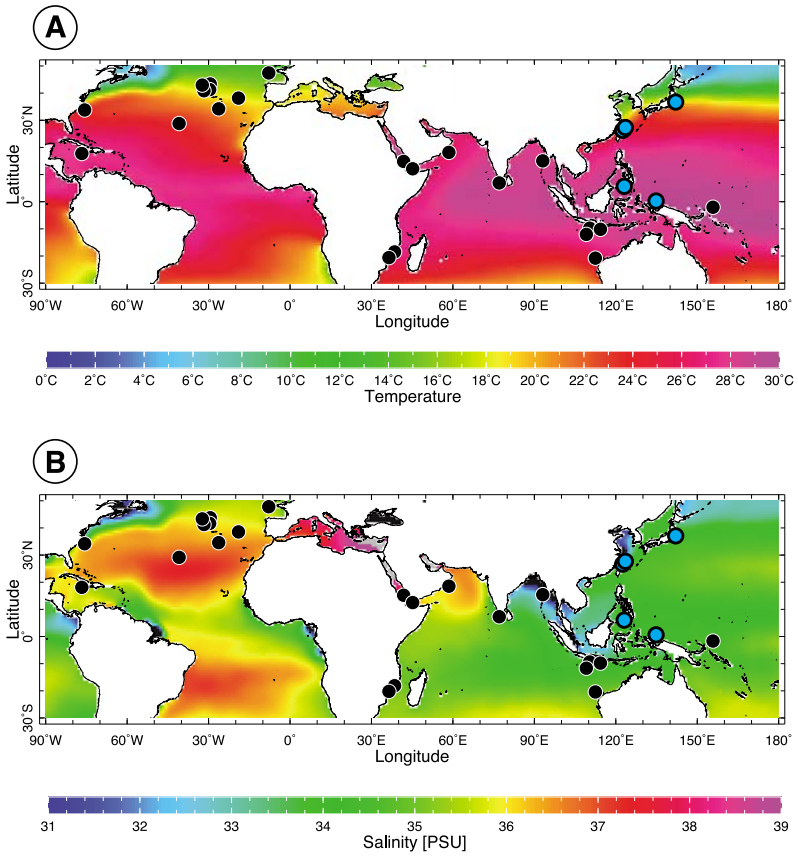

Figure 1. Sample location maps. (a) Sample locations are plotted on a map showing the distribution of annual mean sea surface temperatures [*Locarnini et al.*, 2006]. (b) Sample locations are plotted on a map showing the distribution of annual mean sea surface salinities [*Antonov et al.*, 2006]. Core tops are shown as black circles. Plankton tow samples are represented by blue circles.

3.1. Oxygen Isotopic Analyses

[14] Oxygen isotopic ratios were obtained on 6 to 30 shells. Shells were ultrasonically cleaned in a methanol bath to remove clays and other impurities. They were roasted under vacuum at 380°C during 45 min to eliminate organic matter. Samples were analyzed with a Finnigan Δ+ mass spectrometer. All results are expressed as $\delta^{18}O$ in ‰ versus V-PDB with respect to NBS 19 and NBS 18 standards. The analytical reproducibility as determined from replicate measurements of a carbonate standard is ±0.05‰ (1σ). The mean standard deviation of replicate *G. ruber* analyses is ∼0.11‰ (RSD = 4%).

3.2. Mg/Ca Analyses

[15] About 20–30 specimens per sample were used for each Mg/Ca measurement. Prior to analysis, samples were cleaned following the procedure of *Barker et al.* [2003], which includes several ultrasonic treatments in water then ethanol to remove adhesive clays, and then a reaction with alkali buffered 1% hydrogen peroxide at 100°C to remove any organic matter. A very slight acid leaching with 0.001 M nitric acid was finally applied to eliminate contaminants adsorbed on foraminiferal tests. Analyses were performed on a Varian Vista Pro Inductively Coupled Plasma Atomic Emission Spectrometer (ICP-AES) following the intensity ratio method of *de Villiers et al.* [2002]. Potential contamination by silicates was checked by looking at Fe, Al and Mn concentrations. All samples showed Fe/Mg < 0.1 mol mol^{-1} and we observed no correlation between Mg/Ca and either Fe/Ca or Al/Ca, clearly indicating the lack of significant contamination by silicates. The

Table 1b. Plankton Tow Locations

Area	Plankton Tow	Latitude	Longitude
West Pacific	MD122-PT10	0°15.88′N	134.14.55′E
West Pacific	MD122-PT12	6°43.79′N	122°54.86′E
West Pacific	MD122-PT17	24°49.68′N	122°37.24′E
West Pacific	MD122-PT18	25°20.45′N	122°28.69′E
West Pacific	MD122-PT26	36°07.22′N	141°53.50′E

mean external reproducibility of a standard solution of Mg/Ca = 5.23 mmol mol^{-1} is ±0.5% (RSD). The average Mg/Ca reproducibility of replicate *G. ruber* analyses is ±0.18 mmol mol^{-1} (1σ).

4. Temperature Estimates

4.1. Mg/Ca Temperatures

[16] The Mg/Ca of *G. ruber* were converted to temperatures ($T_{Mg/Ca}$) based on *Anand et al.*'s [2003] empirical equation for *G. ruber* in the size fraction 250–350 μm:

$$T_{Mg/Ca} = \frac{\ln\left(\frac{(Mg/Ca)}{0.449}\right)}{0.09} \quad (1)$$

[17] Propagation of analytical and calibration errors results in a ±1°C uncertainty on $T_{Mg/Ca}$ estimates.

[18] We chose to use *Anand et al.*'s [2003] Mg/Ca thermometry equation for two reasons. First, recent interlaboratory comparisons have clearly shown that Mg/Ca results are dependant on the procedure used to clean foraminiferal shells [*Rosenthal et al.*, 2004]. *Anand et al.* [2003] used the cleaning procedure from *Barker et al.* [2003], which is the procedure we also adopted for this study. The Mg/Ca thermometry regression equation obtained by *Anand et al.* [2003] appears to be fully coherent, therefore, with our own data set. In addition, *Anand et al.*'s [2003] regression equation for $T_{Mg/Ca}$ thermometry of *G. ruber* was developed from a sediment trap series located in a single area (the Sargasso Sea), which insures that only little bias may be expected from other hydrographic variations than sea surface temperature (i.e., SSS).

4.2. Isotopic Temperatures

[19] In the Arabian Sea, sediment trap series indicate that *G. ruber* would virtually record mean annual sea surface hydrographic conditions [*Curry et al.*, 1992; *Conan and Brummer*, 2000; *Peeters et al.*, 2002]. However, this may not be true for other areas covered by our database. The paucity of information about the seasonality of *G. ruber* productivity makes it difficult to compare directly $T_{Mg/Ca}$ and SST derived from a modern hydrographic atlas. Thus, in order to get a reference temperature to which $T_{Mg/Ca}$ can be compared, we estimated the calcification temperature of *G. ruber* from $\delta^{18}O$ measurements.

[20] *G. ruber s.s.* is a surface dwelling species (0–30 m water depth) which calcifies at isotopic equilibrium with ambient seawater [*Duplessy et al.*, 1991; *Wang et al.*, 1995]. The isotopic temperature of calcification (T_{iso}) is dependant on the oxygen isotopic composition of seawater ($\delta^{18}O_{sw}$), and can be obtained from the measured $\delta^{18}O$ of *G. ruber* ($\delta^{18}O_f$) using the isotopic temperature equation of *Shackleton* [1974]:

$$T_{iso} = 16.9 - 4.38 * \left(\delta^{18}O_f + 0.27 - \delta^{18}O_{sw}\right) + 0.1 * \left(\delta^{18}O_f + 0.27 - \delta^{18}O_{sw}\right)^2 \quad (2)$$

[21] In order to calculate T_{iso}, we need to estimate surface $\delta^{18}O_{sw}$ at our sites. For this purpose, we have used the gridded $\delta^{18}O_{sw}$ atlas derived by *LeGrande and Schmidt* [2006]. These authors have devoted a great deal of effort in interpolating the seawater $\delta^{18}O_{sw}$ data available to produce an internally consistent $\delta^{18}O_{sw}$ gridded atlas. In the Indian Ocean, for instance, the Root Mean Square of the differences between atlas interpolated and GEOSECS $\delta^{18}O_{sw}$ measurements is 0.1‰ [*LeGrande and Schmidt*, 2006].

[22] Since we do not know if *G. ruber* can present a seasonal productivity over some areas, we checked what maximum uncertainty would result on the estimated T_{iso} when using mean annual $\delta^{18}O_{sw}$ values instead of seasonally weighted $\delta^{18}O_{sw}$ values. Hydrographic data obtained from *Antonov et al.* [2006] and averaged over the 0–30 m water depth interval, show that absolute differences between the annual mean SSS and seasonal extremes at all of our sites, except three, are <0.4 psu (ranging from −0.3 to +0.3 psu, with an average absolute value of 0.16 psu). Based on regional $\delta^{18}O_{sw}$-SSS empirical relationships [*LeGrande and Schmidt*, 2006], the absolute maximum difference between annual mean $\delta^{18}O_{sw}$ and seasonal $\delta^{18}O_{sw}$ at our sites is therefore ≤0.09‰ (average = 0.03‰), which is smaller than the uncertainty on the analytical measurements of *G. ruber* $\delta^{18}O$. Thus, the annual $\delta^{18}O_{sw}$ value obtained from the gridded atlas of *LeGrande and Schmidt* [2006] appears to be a valid choice for those sites with seasonal salinity variations <0.3 psu. It introduces a maximum T_{iso} shift ≤0.5°C (average over our database = 0.3°C) relative to seasonally weighted estimations.

[23] At three sites, however, SSS variations over the course of the year are much higher, reaching up to 0.8 psu. This is the case at the Red Sea site (core MD92-1008), at the southern tip of India (core

Table 2a. Hydrographic Parameters at the Location of Core Top and Geochemical Data Obtained on *G. ruber*[a]

Core Top	SSS (‰)	$\delta^{18}O_{sw}$ (‰)	$\delta^{18}O_f$ (‰)	T_{iso} (°C)	Mg/Ca (mmol mol^{-1})	$T_{Mg/Ca}$ (°C)	ΔT (°C)	$Mg/Ca_{(T)}$ (mmol mol^{-1})	$\Delta Mg/Ca_{(s)}$ (mmol mol^{-1})
INMD48BX.1	36.96	1.19	−0.48	23.2	4.59	25.8	2.6	3.63	0.96
INMD68BX.6	36.47	1.04	−0.27	21.6	3.61	23.2	1.6	3.13	0.48
MD952038	36.23	0.94	−0.12	20.4	2.84	20.5	0.1	2.82	0.02
paleo SU 9007P	35.98	0.78	−0.05	19.4	3.02	21.2	1.8	2.57	0.45
paleo SU 9004P	36.03	0.81	−0.42	21.2	3.33	22.3	1.1	3.03	0.30
paleo SU 9002P	36.03	0.83	−0.06	19.6	3.20	21.8	2.2	2.63	0.57
paleo SU 9003P	36.09	0.84	−0.27	20.7	3.00	21.1	0.4	2.88	0.12
paleo SU 9008P	35.89	0.74	−0.29	20.3	3.04	21.3	1.0	2.78	0.26
paleo SU 9006P	35.98	0.78	0.00	19.2	2.96	21.0	1.8	2.51	0.45
CHO 288-54	35.72	0.82	−2.06	29.0	5.35	27.5	−1.5	6.11	−0.76
MD95-2002	35.52	0.56	0.34	16.7	2.09	17.1	0.4	2.01	0.08
MD99-2203	35.99	0.72	−1.42	25.4	4.43	25.4	0.0	4.42	0.01
MD79-255	35.04	0.44	−1.90	26.4	3.96	24.2	−2.2	4.83	−0.87
MD79-257	35.10	0.44	−1.81	26.0	4.23	25.0	−1.0	4.65	−0.42
MD92-1002	36.29	0.77	−1.76	27.3	5.43	27.7	0.4	5.24	0.19
MD00-2359 PC	34.15	0.26	−2.44	28.1	4.73	26.1	−2.0	5.66	−0.93
MD 98-2165	34.10	0.28	−2.59	29.0	4.80	26.3	−2.7	6.09	−1.29
MD77-176	32.57	−0.10	−3.02	29.2	4.70	26.1	−3.1	6.23	−1.52
MD00-2360top	35.00	0.42	−1.71	25.4	4.58	25.8	0.4	4.40	0.18
MD92-1008	36.49	0.50	−1.86	26.5	6.54	29.8	3.3	4.88	1.66
MD002358top	34.36	0.31	−1.97	26.1	3.69	23.4	−2.7	4.71	−1.02
MD00-2359 G	34.15	0.26	−2.70	29.4	4.66	26.0	−3.4	6.34	−1.69
ODP117-723	36.10	0.61	−2.25	28.9	6.85	30.3	1.4	6.05	0.80
MD77-191	34.73	0.25	−2.44	28.1	5.13	27.1	−1.0	5.62	−0.49
ERDC92BX	34.46	0.27	−2.44	28.2	5.07	26.9	−1.2	5.67	−0.60

[a] SSS and $\delta^{18}O_{sw}$ are extracted from *Antonov et al.* [2006] and *LeGrande and Schmidt* [2006], respectively. Values of $\delta^{18}O_f$ were measured on *G. ruber*, and the isotopic temperature (T_{iso}) was calculated using an equation from *Shackleton* [1974]. Values of Mg/Ca were measured on *G. ruber*, and the corresponding temperatures ($T_{Mg/Ca}$) were calculated based on calibration from *Anand et al.* [2003] for *G. ruber* in the size fraction 250–350 μm. Atlantic ocean data are from *Cléroux* [2007], and Indo-Pacific data are from *Levi* [2003] and *Mathien-Blard* [2008]. ΔT is the difference between $T_{Mg/Ca}$ and T_{iso}. $Mg/Ca_{(T)}$ is the Mg/Ca that is estimated by injecting T_{iso} in the calibration from *Anand et al.* [2003]. $\Delta Mg/Ca_{(s)}$ is the difference between those estimated $Mg/Ca_{(T)}$ values and the measured Mg/Ca values (see section 5.4 for details).

MD77-191) and in the Bay of Bengal (core MD77-176). For those sites, we extracted seasonal SSS and converted them to $\delta^{18}O_{sw}$ using regional $\delta^{18}O$-SSS relationships [*LeGrande and Schmidt*, 2006]. We then looked for the season which resulted in the best match between calcification T_{iso} and the SST from *Locarnini et al.* [2006]. The highest concordance between atlas-derived SST and T_{iso} for the Red Sea site (core MD92-1008) is obtained with winter SSS and SST. *G. ruber* is a species which is found over a relatively large range of sea surface temperatures and salinities [*Zaric et al.*, 2005], still the temperature and salinity conditions of the winter season at our Red Sea site (SST = 25.5°C; SSS = 36.5 psu) are probably more suitable for *G. ruber* growth than the extreme values reached during the summer season (SST = 31.5°C; SSS = 37.6 psu). In addition, the northeast monsoon winds induce strong chlorophyll (Chl) development near the Bab-El-Mandeb Strait during winter (NASA-SeaWifs; http://oceancolor.gsfc.nasa.gov/cgi/browse.pl). This may possibly promote higher plankton foraminifera development at this season. For the Bay of Bengal (core MD77-176) and south of India (core MD77-191) sites, the best match between seasonal atlas SST values and estimated T_{iso} is obtained for the spring.

5. Results

[24] Results for Mg/Ca and $\delta^{18}O_f$ analyses performed on core tops are summarized in Table 2a. Mg/Ca ranges from 2.09 mmol mol^{-1} to 6.85 mmol mol^{-1}. The highest Mg/Ca values are obtained for core tops located in high-salinity areas (e.g., Red Sea, Arabian Sea, southern tip of India). A statistically significant linear relationship is obtained by plotting $T_{Mg/Ca}$ relative to T_{iso} (R^2 = 0.81; Figure 2a). However, if we go into details and take into account the data by oceanic sectors, it is striking that no relationship is observed for Indo-Pacific core tops (Figure 2b; linear regression gives a R^2 of 0.12 only).

5.1. Indo-Pacific Core Top Data

[25] In order to separate a potential bias effect from the true temperature effect in the Indo-Pacific

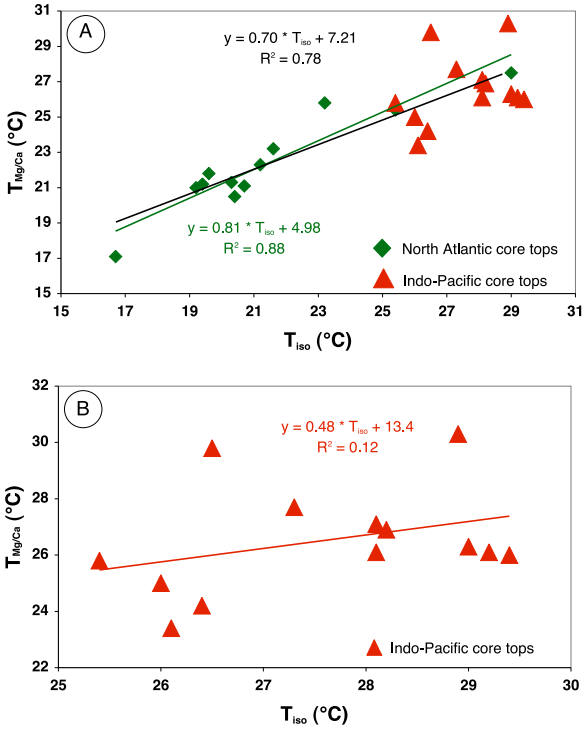

Figure 2. (a) *Globigerinoides ruber* T_{iso} ($\delta^{18}O$-derived isotopic temperature) plotted against $T_{Mg/Ca}$ for the Atlantic (green diamonds) and Indo-Pacific (red triangles) core tops. The linear regression derived from taking into account all core top data is shown in black. The green line corresponds to the linear regression obtained with North Atlantic core tops only. (b) T_{iso} plotted against $T_{Mg/Ca}$ for the Indo-Pacific core tops only, with the corresponding linear regression.

region, we estimated at each site the difference (ΔT) between potentially biased $T_{Mg/Ca}$ and our reference, isotopic temperature (ΔT = $T_{Mg/Ca}$ minus T_{iso}). ΔT varies from −3.4°C in the West Pacific to +3.3°C in the Red Sea, with a Root Mean Square (RMS) of 1.9°C. We first checked the potential bias on $T_{Mg/Ca}$ caused by surface water [CO_3^{2-}] by plotting ΔT relative to carbonate ion data extracted from *Archer*'s [1996] gridded database and averaged over the 0–30 m water depth interval. No correlation is observed (R^2 = 0.01). This confirms the results of *G. ruber* culture experiments, which indicate that Mg/Ca is not affected by carbonate ion at ambient seawater [CO_3^{2-}] concentrations [*Kisakürek et al.*, 2008]. ΔT shows, on the other hand, a strong, positive linear correlation with sea surface salinity in the Indo-Pacific region (Figure 3a; correlation coefficients R^2 = 0.72):

$$\Delta T = 1.57 * SSS - 55.7 (R^2 = 0.72) \quad (3)$$

5.2. Atlantic Ocean Core Top Data

[26] For our Atlantic Ocean core top samples, ΔT varies from −1.5°C to 2.6°C, with a RMS of 1.2°C. As was concluded for the Indo-Pacific data set, no significant correlation is observed between ΔT and surface water [CO_3^{2-}] concentrations (R^2 = 0.17). ΔT from Atlantic core tops overlap well with those from Indo-Pacific data when plotted versus SSS (Figure 3b). Thus, although *G. ruber* $T_{Mg/Ca}$ from Atlantic core tops did correlate relatively well with the isotopic temperatures, T_{iso} (Figure 2a), it is reasonable to conclude that both Indo-Pacific and Atlantic *G. ruber* $T_{Mg/Ca}$ are salinity-biased to some extent. As far as the Atlantic Ocean is concerned, the salinity effect on *G. ruber* $T_{Mg/Ca}$ does not strongly obliterate the correlation with T_{iso} because of the small surface salinity range covered by our *G. ruber* data set in this area (35.5 to 37 psu). In the Indo-Pacific region, on the other hand, our data set covers a much larger salinity range (32.6 to 36.5 psu), explaining why the salinity has a more visible effect on $T_{Mg/Ca}$ and produces such a strong discrepancy with calcification temperature obtained from oxygen isotopes T_{iso}.

5.3. Plankton Tow Data

[27] The salinity effect on Mg incorporation was confirmed by looking at *G. ruber* $T_{Mg/Ca}$ obtained from five plankton tows retrieved in the Indonesian Archipelago and the western Pacific during IMAGES cruise VII [*Bassinot et al.*, 2002]. Sea surface temperatures and salinities were measured during the cruise, which makes it possible to directly compare $T_{Mg/Ca}$ with in situ temperatures at the locations where *G. ruber* calcified. Over the studied area, which is characterized by low SSS (ranging from 33.4 to 34.4 psu), the estimated $T_{Mg/Ca}$ are systematically lower than the in situ SST (Table 2b). The RMS of the differences (ΔT = $T_{Mg/Ca}$ − T_{insitu}) is 2.7°C (with values ranging from −1.7 to −3.6°C). These ΔT are plotted versus in situ salinities on the same graph than the core top data (Figure 3b). As can be readily seen from Figure 3b, the plankton data overlap well with core top data, clearly confirming the strong bias of salinity on the Mg/Ca thermometer and indicating that our core top Mg/Ca data were not biased by diagenetic effects.

5.4. Synthesis: Salinity Effect on *G. ruber* Mg/Ca

[28] A simple linear regression obtained from the 25 core tops and the 5 plankton tows shows a

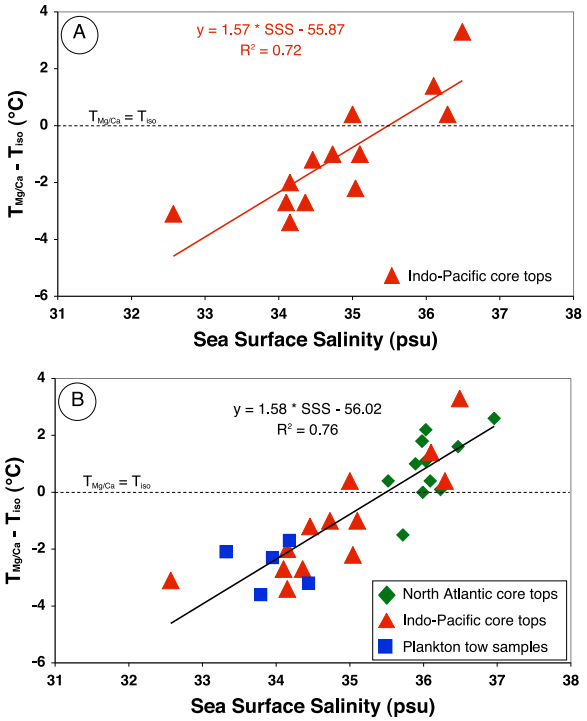

Figure 3. (a) ΔT (= $T_{Mg/Ca}$ − T_{iso}) plotted against atlas-derived sea surface salinities [*Antonov et al.*, 2006] for the Indo-Pacific core tops. (b) ΔT (= $T_{Mg/Ca}$ − T_{iso}) plotted against atlas-derived sea surface salinities [*Antonov et al.*, 2006] for the Indo-Pacific core tops (red triangles) and North Atlantic core tops (green diamonds). On the same graph are also plotted ΔT (= $T_{Mg/Ca}$ − in situ T) for plankton tow data (blue squares). The linear regression equation was calculated using all the data on the graph.

good correlation coefficient between ΔT and SSS ($R^2 = 0.76$):

$$\Delta T = 1.58 * SSS - 56 \left(R^2 = 0.76\right) \quad (4)$$

Kisakürek et al. [2008] have observed an exponential effect of salinity on Mg/Ca temperature. As far as our core top data set is concerned, however, an exponential fit would not have resulted in a better correlation coefficient than a simple linear regression ($R^2 = 0.76$ in both cases). We preferred, therefore, to use a simple linear regression as this proves to be easier to handle in the development of a correction procedure for past temperature reconstructions (see below).

[29] The slope of this linear relationship indicates that 1 psu change in salinity would induce a ~1.6°C change in $T_{Mg/Ca}$ relative to the isotopic temperature of calcification. It is interesting to note that ΔT equals 0 ($T_{iso} = T_{Mg/Ca}$) for a salinity of ~35.4 psu, which means that Mg/Ca thermometry of *G. ruber* using *Anand et al.*'s [2003] calibration is virtually unbiased for sea surface salinities that are close to the average surface ocean salinity. Below ~35.4 psu, $T_{Mg/Ca}$ are lower than T_{iso}, and they are higher than T_{iso} for salinities above ~35.4 psu.

[30] Using either T_{iso} (for core top material) or T_{insitu} (for plankton tow samples) as our best estimates of *G. ruber* calcification temperatures, we can use *Anand et al.*'s [2003] equation (5) to estimate the values of *G. ruber* Mg/Ca that should be expected from a temperature effect only (Mg/Ca_T):

$$Mg/Ca_T = 0.449 * \exp(0.09 * T) \quad (5)$$

[31] The impact of salinity on *G. ruber* Mg/Ca ($\Delta Mg/Ca_S$) can be simply obtained by substracting the calculated Mg/Ca_T values to the actual Mg/Ca measured on *G. ruber* ($\Delta Mg/Ca_S = Mg/Ca_{(measured)} - Mg/Ca_T$) (Figure 4). Although an exponential regression can be fit to the data, it does not result in a better correlation coefficient than a simple linear

Table 2b. Hydrographic Parameters at the Location of Plankton Tow Samples and Geochemical Data Obtained on *G. ruber*[a]

Plankton Tow	In Situ SSS (‰)	In Situ SST (°C)	Mg/Ca (mmol mol^{-1})	$T_{Mg/Ca}$ (°C)	ΔT (°C)	$Mg/Ca_{(T)}$ (mmol mol^{-1})	$\Delta Mg/Ca_{(s)}$ (mmol mol^{-1})
MD122-PT10	34.18	29.5	5.46	27.8	−1.7	6.39	−0.93
MD122-PT12	33.32	29.9	5.49	27.8	−2.1	6.62	−1.13
MD122-PT17	33.79	28.2	4.12	24.6	−3.6	5.68	−1.56
MD122-PT18	33.95	26.2	3.85	23.9	−2.3	4.75	−0.90
MD122-PT26	34.44	24.1	2.94	20.9	−3.2	3.93	−0.99

[a] SSS and SST were measured in situ during WEPAMA cruise of R/V *Marion Dufresne* [*Bassinot et al.*, 2002]. Values of Mg/Ca were measured on *G. ruber*, and the corresponding temperatures ($T_{Mg/Ca}$) were calculated based on calibration from *Anand et al.* [2003] for *G. ruber* in the size fraction 250–350 μm. Atlantic ocean data are from *Cléroux* [2007], and Indo-Pacific data are from *Levi* [2003] and *Mathien-Blard* [2008]. ΔT is the difference between $T_{Mg/Ca}$ and in situ temperatures. $Mg/Ca_{(T)}$ is the Mg/Ca that is estimated by injecting in situ temperatures in the calibration from *Anand et al.* [2003]. $\Delta Mg/Ca_{(s)}$ is the difference between those estimated $Mg/Ca_{(T)}$ values and the measured Mg/Ca values (see section 5.4 for details).

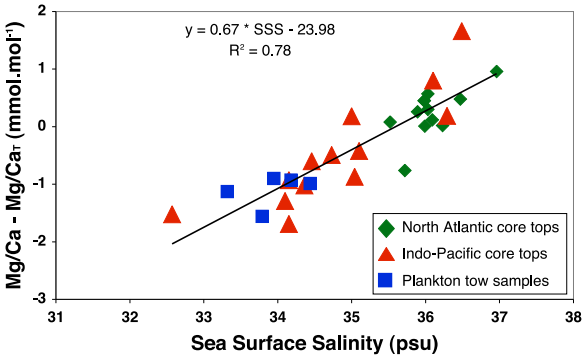

Figure 4. Residual Mg/Ca ($\Delta Mg/Ca_s$; see section 5.4) plotted against atlas-derived sea surface salinity [*Antonov et al.*, 2006]. Indo-Pacific core tops are symbolized by red triangles, North Atlantic core tops are shown as green diamonds, and plankton tow samples are represented by blue squares. The black line materializes the linear regression calculated taking into account all the data on the graph.

regression. The linear regression between $\Delta Mg/Ca_S$ and SSS results in the following equation:

$$\Delta Mg/Ca_S = 0.67 * SSS - 24 (R^2 = 0.78) \quad (6)$$

[32] The slope of this relationship indicates that a SSS change of 1 psu induces a ΔMg/Ca change of 0.67 mmol mol^{-1} (which corresponds to a 15% change in Mg/Ca per psu when considering the Mg/Ca values that were measured on our core tops).

6. Discussion

6.1. Salinity Effect on *G. ruber* Mg/Ca: Discrepancy Between Core Top and Culture Studies

[33] Our results on *G. ruber* confirm the positive relationship between planktonic foraminiferal Mg/Ca and salinity that was suggested by several authors [*Lea et al.*, 1999; *Nürnberg et al.*, 1996]. The ~15% Mg/Ca increase per psu that we observe is slightly higher than the 11% change per psu established for *G. sacculifer* from laboratory cultures [*Nürnberg et al.*, 1996], but is much higher than the salinity sensitivity observed for *O. universa* (~4% Mg/Ca change per psu [*Lea et al.*, 1999]). More surprisingly, the salinity effect that we observe is also about three times stronger than what has been deduced recently from *G. ruber* culture experiments (~5% Mg/Ca change per psu [*Kisakürek et al.*, 2008]). The Mg/Ca sensitivity to salinity that is deduced from *G. ruber* culture experiments [*Kisakürek et al.*, 2008] is clearly too small to account for the large differences between Mg/Ca- and δ^{18}O-derived temperatures in our core top and plankton tow database.

[34] Some additional work is required to address this discrepancy between *G. ruber* core top and plankton tow results, in the one hand, and culture study results, in the other hand. Does this discrepancy simply reflect the fact that culture experiments create a stress on *G. ruber* individuals, which alters somewhat the calcification processes and masks the real sensitivity of Mg incorporation to salinity? Could this discrepancy indicate that Mg incorporation evolves across the course of *G. ruber* lifetime? The *G. ruber* specimens retrieved from core top sediments and plankton tows have presumably grown their entire shell at the same sea surface conditions. In the culture experiment, however, the salinity effect on Mg/Ca can only be addressed through the analysis of the last *G. ruber* chambers, which calcified during the course of the experiment. Thus, the weaker salinity effect on *G. ruber* Mg/Ca that is deduced from culture experiments [*Kisakürek et al.*, 2008] may indicate that during the later stages of *G. ruber* shell development, the incorporation of Mg in the calcite lattice is less affected by salinity than during the early stages.

6.2. Salinity Effect on the *G. ruber* Mg/Ca Paleothermometer

[35] Our data show that the temperature offset (ΔT) between *G. ruber* $T_{Mg/Ca}$ and T_{iso} in the North Atlantic, and in the tropical Indian and western Pacific Oceans is a function of salinity, over the range [~32–37 psu] covered by our database (with virtually no effect on Mg/Ca thermometry for a salinity around ~35.4‰ when using *Anand et al.*'s [2003] calibration). This has important implications when calibrating Mg/Ca thermometry using core top data from remote ocean locations with different SSS, and it has also crucial implications when using foraminiferal Mg/Ca for paleoceanographic reconstructions. During the Last Glacial Maximum, for instance, the average ocean salinity was ~1.15 psu higher than today due to the storage of freshwater in the continental ice sheets [*Adkins et al.*, 2002]. According to our results, and regardless of possible local changes in evaporation/precipitation budgets, SST obtained from the *G. ruber* Mg/Ca would be potentially biased by up to ~1.6°C, if the effect of the global change in salinity was not corrected for. This represents a large difference, especially in view of the puzzling

discrepancies that still exist between available sea surface temperature reconstructions obtained with other temperature proxies, or with temperature estimates obtained on land [e.g., *Thompson et al.*, 1995; *Bard et al.*, 1997; *Beck et al.*, 1997; *Guilderson et al.*, 2001; *Chen et al.*, 2005]. In addition, estimates of past sea surface $\delta^{18}O_{sw}$ obtained from coupled $\delta^{18}O_f$ and $T_{Mg/Ca}$ measurements will be biased as well.

6.3. Development of a Correction for *G. ruber* SST and $\delta^{18}O_{sw}$ Estimates

[36] Our goal was to develop a correction procedure that could be easily applied to $T_{Mg/Ca}$ and $\boldsymbol{\delta}^{18}O_f$ measured on *G. ruber* in order to derive sea surface temperature and $\delta^{18}O_{sw}$ corrected for the salinity effect on Mg/Ca. For such a correction approach, past SSS are not known, but SSS and $\delta^{18}O_{sw}$ are tightly linked, which makes it possible to address the salinity effect for paleoreconstructions. Two aspects have to be taken separately into account (as the slopes are rather different). These are: 1/ the global SSS-$\delta^{18}O_{sw}$ evolution induced by waxing/waning of the continental ice sheets, and 2/ the regional SSS-$\delta^{18}O_{sw}$ relationship controlled by evaporation/precipitation mechanisms and continental runoff. In order to differentiate between these two processes, past SSS is expressed as the sum of modern surface salinity (S_0), a local change in salinity related to changes in evaporation/precipitation budget (ΔS_l) and the global change in salinity induced by waxing and waning of ice sheets (ΔS_g):

$$SSS = S_0 + \Delta S_l + \Delta S_g \quad (7)$$

[37] Then, each term of this equation can be expressed as a function of seawater $\delta^{18}O$ change, either local ($\Delta\delta^{18}O_l$) or global ($\Delta\delta^{18}O_g$). In the following paragraph, we will present and discuss the data available for setting up these global and local SSS-$\delta^{18}O_{sw}$ relationships.

[38] The most accurate constraints on the global $\delta^{18}O$ change ($\Delta\delta^{18}O_g$) induced by the waxing and waning of continental ice sheets are provided by high-resolution records of benthic foraminifer $\delta^{18}O$ in the high-latitude oceans [*Labeyrie et al.*, 1987; *Duplessy et al.*, 2002]. These authors showed that the $\delta^{18}O$ of seawater in the deep ocean during the LGM was 1.05 ± 0.20‰ heavier than today. As for the global salinity change (ΔS_g), it can be estimated based on today's average ocean water depth (3800 m) and assuming a −125 m glacioeustatic drop in sea level at the LGM from Barbados corals [*Fairbanks*, 1989]. Based on the true hypsometry of the modern ocean, this sea level drop at the LGM results in a ~1.15 psu salinity increase (a LGM value of 35.85 psu for a modern salinity of 34.7 psu [*Adkins et al.*, 2002]). Thus, global salinity (ΔS_g) and $\delta^{18}O$ ($\Delta\delta^{18}O_g$) changes from the LGM to the modern can be linearly related as follows:

$$\Delta S_g = 1.1 * \Delta\delta^{18}O_g \quad (8)$$

[39] Let us now look at the local SSS-$\delta^{18}O_{sw}$ relationships. As indicated above, evaporation/precipitation budget and continental runoff lead to strong, regional SSS-$\delta^{18}O_{sw}$ relationships. Because paleo-SSS cannot be reconstructed independently from paleo-$\delta^{18}O_{sw}$ in marine sedimentary records, we are not able to reconstruct past SSS-$\delta^{18}O_{sw}$ relationships. Thus, several paleoceanographers have used the modern, regional SSS-$\delta^{18}O_{sw}$ relationships to infer past changes in SSS from pelagic carbonate $\delta^{18}O$ measurements [*Broecker and Denton*, 1989; *Duplessy et al.*, 1991; *Rostek et al.*, 1993]. Yet, *Rohling and Bigg* [1998] pointed out that these regional SSS-$\delta^{18}O_{sw}$ relationships may have changed in the past. Therefore, the question remains: can we use such modern relationships to tie regional changes in SSS and $\delta^{18}O_{sw}$ in our correction procedure and what uncertainties would this approach lead to?

[40] As far as the tropical Indian Ocean is concerned, *Delaygue et al.* [2001] have computed the SSS-$\delta^{18}O_{sw}$ relationship at the LGM by running a two-dimensional array of box model for surface water hydrography, using atmospheric fluxes estimated by the atmospheric general circulation model of NASA/Goddard Institute for Space Studies (GISS). Delaygue et al.'s coupled, multibox model does not show any clear change for the $\delta^{18}O_{sw}$-salinity relationship at LGM compared to today, in either the Arabian Sea or the Bay of Bengal. In the Arabian Sea, the estimated LGM slope of the $\delta^{18}O_{sw}$-salinity relationship is similar to the modern observed one. In the Bay of Bengal, when taking into account runoff effects, the estimated slope at the LGM ranges between 0.15 and 0.20 (accounting for the global oceanic $\delta^{18}O_{sw}$ and salinity enrichments). This computed range compares well with the modern, observed slope (0.18 [*Delaygue et al.*, 2001]). *Delaygue et al.*'s [2001] results seem to indicate, therefore, that it is reasonably safe to use modern $\delta^{18}O_{sw}$-salinity relationships in our correction procedure for the tropical Indian Ocean.

Table 3. Equation Parameters Used to Derive Unbiased Seawater $\delta^{18}O_{sw}$ From Mg/Ca Temperature and $\delta^{18}O_f$ of *G. ruber* in Different Oceanic Regions[a]

Area	A	B	C	D
Tropical Indian Ocean	−71.0	196.8	−4.0	3.3
Arabian Sea	−52.0	102.7	−2.4	1.7
Red Sea	−47.1	82.9	−2.0	1.3
North Atlantic Ocean	−36.0	46.1	−1.1	0.5
Tropical Atlantic Ocean	−74.3	217.5	−4.2	3.5
Mediterranean Sea	−49.8	94.6	−2.3	1.6
Tropical Pacific Ocean	−50.9	98.9	−2.3	1.6

[a] The equation is of the form: $\delta^{18}O_{sw}* = \delta^{18}O_f + A + 5*(B + 0.4\ T_{Mg/Ca} + C\delta^{18}Oc + D\Delta\delta^{18}O_g)^{\wedge 0,5}$. See section 6.3 for details.

[41] Similar modeling approach would be needed to test the stability though time of the SSS-$\delta^{18}O_{sw}$ relationships in other areas of the world ocean. It is likely that, in specific areas, significant changes can be expected. This should be the case for the Red Sea, for instance. The Red Sea is a semi-enclosed basin and the SSS-$\delta^{18}O_{sw}$ relationship there is strongly dependant upon water fluxes exchanged with the Arabian Seawaters through the shallow Bal-El-Mandeb sill. Those fluxes have likely changed at the glacial-interglacial time scale as a result of glacioeustatic sea level changes. Thus, a correction procedure that would assume a constant SSS-$\delta^{18}O_{sw}$ relationship through time could only be applied over the Holocene but will not be valid for periods over which sea level changes had modified significantly the water exchanges with the Arabian Sea.

[42] In the following part, we will detail, for the tropical Indian Ocean, the correction procedure we developed to get unbiased paleo-SST and $\delta^{18}O_{sw}$ from *G. ruber* $T_{Mg/Ca}$ and $\delta^{18}O_f$ measurements. In Table 3, correction equations are given for other areas of the world ocean (based on regional SSS-$\delta^{18}O_{sw}$ relationships from *Legrande and Schmidt* [2006]). Those correction equations should be used with care, keeping in mind that our approach assumes that regional SSS-$\delta^{18}O_{sw}$ relationships have not changed over the past, an assumption that might prove significantly wrong over specific areas.

[43] In the tropical Indian Ocean, the $\delta^{18}O$-SSS relationship compiled by *LeGrande and Schmidt* [2006] is:

$$\delta^{18}O_{sw} = 0.16 * SSS - 5.31 \quad (9)$$

[44] Combining (7) with equations (8) and (9), we can express SSS as a function of modern surface $\delta^{18}O_{sw}$ ($\delta^{18}O_{sw0}$), and the local and global changes in $\delta^{18}O$ ($\Delta\delta^{18}O_l$ and $\Delta\delta^{18}O_g$, respectively):

$$SSS = \left(\delta^{18}O_{sw0} + 5.31\right)/0.16 + \Delta\delta^{18}O_l/0.16 + 1.1 * \Delta\delta^{18}O_g \quad (10)$$

$\delta^{18}O_{sw}$ being the sea surface isotopic composition in the past (= $\delta^{18}O_{sw0} + \Delta\delta^{18}O_l + \Delta\delta^{18}O_g$), equation (10) can be rewritten as:

$$SSS = \left(6.25 * \delta^{18}O_{sw}\right) - \left(5.15 * \Delta\delta^{18}O_g\right) + 33.19 \quad (11)$$

[45] Then, replacing SSS in equation (4) by its expression (11), we come up with an equation in which T_{iso} is as a function of $T_{Mg/Ca}$, $\delta^{18}O_{sw}$ and $\Delta\delta^{18}O_g$:

$$T_{iso} = T_{Mg/Ca} - \left(9.88 * \delta^{18}O_{sw}\right) + \left(8.14 * \Delta\delta^{18}O_g\right) + 3.56 \quad (12)$$

[46] Using the isotopic paleothermometer equation (2), together with equation (12), we have now a set of two independent equations with two unknowns: $\delta^{18}O_{sw}$ and T_{iso}. These equations are combined and resolved, which allows to extract a $\delta^{18}O_{sw}$ term which is virtually "corrected" for the salinity effect on $T_{Mg/Ca}$ ($\delta^{18}O_{sw}$*):

$$\delta^{18}O^*_{sw} = \delta^{18}O_f - 71.0 + 5 * \left(196.8 + \left(0.4 * T_{Mg/Ca}\right) + \left(3.3 * \Delta\delta^{18}O_g\right) - \left(4.0 * \delta^{18}O_f\right)\right)^{\wedge 0.5} \quad (13)$$

[47] To solve this equation, we need only the parameters measured on *G. ruber* (namely, $T_{Mg/Ca}$ and $\delta^{18}O_f$), plus an estimate of global seawater $\delta^{18}O$ enrichment relative to modern conditions ($\Delta\delta^{18}O_g$). This global signal can be readily derived from sea level or global, benthic $\delta^{18}O$ records [*Labeyrie et al.*, 1987; *Lambeck and Chappell*, 2001; *Waelbroeck et al.*, 2002].

[48] Finally, in order to obtain a calcification temperature for *G. ruber* that is corrected for the salinity bias, the adjusted $\delta^{18}O_{sw}$* obtained from equation (13) is either reinjected in the original, thermometry equation from *Shackleton* [1974] (equation (2)), or in equation (12).

6.4. Accuracy and Limits of the Correction Procedure

6.4.1. Applying the Correction Procedure to Our Core Top Database

[49] Performing the correction procedure in a "modern condition mode" ($\Delta\delta^{18}O_g$ = 0‰) over

our own core top database, makes it possible to test the internal consistency of the correction procedure on an ideal case, for which there is no assumption made on SSS-$\delta^{18}O_{sw}$ relationships in the past. Since the whole procedure for this "salinity correction" rests, basically, upon an empirical adjustment of *G. ruber*–derived $\delta^{18}O_{sw}$ to modern Atlas $\delta^{18}O_{sw}$ values, it is not surprising that the correspondence between these two sets of data is drastically improved when using our correction procedure. When taking into account the core top data set, the differences between modern Atlas $\delta^{18}O_{sw}$ [*Legrande and Schmidt*, 2006] and uncorrected, *G. ruber*–derived $\delta^{18}O_{sw}$ (using $T_{Mg/Ca}$) have a RMS of 0.3‰ (with values ranging from −0.7 to +0.7‰). The differences between Atlas $\delta^{18}O_{sw}$ and corrected, *G. ruber*–derived $\delta^{18}O_{sw}$* show a RMS dropping to 0.1‰ (with values ranging from −0.17 to 0.22‰).

[50] The same conclusion can be drawn for the corrected calcification temperatures. We observed large differences between T_{iso}, (estimated using $\delta^{18}O_f$ and Atlas $\delta^{18}O_{sw}$) and uncorrected $T_{Mg/Ca}$. The RMS of ΔT (= $T_{Mg/Ca} - T_{iso}$) equals 1.6°C; values ranging from −3.4 to +3.3°C. The correlation is significantly improved when comparing T_{iso} with the salinity-corrected estimate of calcification temperature calculated from $\delta^{18}O_f$ and $T_{Mg/Ca}$. In that case, RMS of differences drops to 0.5°C, with values ranging from −0.8 to +1.0°C.

6.4.2. To What Degree Can Past Changes in SSS-$\delta^{18}O_{sw}$ Relationships Affect the Correction Procedure?

[51] Our correction procedure is based on the assumption that regional (evaporation/precipitation) and global (ice sheet) SSS-$\delta^{18}O_{sw}$ relationships are known and invariant over the glacial/interglacial cycle (at least, since the LGM). However, some authors have claimed that the regional SSS-$\delta^{18}O_{sw}$ relationships may have changed in the past [e.g., *Rohling and Bigg*, 1998]. Such changes would obviously bias our correction procedure. Thus, we performed sensitivity tests to look at the shift on estimated $\delta^{18}O_{sw}$* and corrected temperatures that would result from using different slopes for either the global or regional SSS-$\delta^{18}O_{sw}$ relationships.

[52] Taking into account uncertainties for the estimated global $\delta^{18}O$ change at the LGM relative to modern (+1.05 ± 0.20‰ [*Labeyrie et al.*, 1987; *Duplessy et al.*, 2002]), the slope of the global glacial/interglacial SSS-$\delta^{18}O$ relationship ($\Delta SSS_g/\Delta\delta^{18}O_g$) can vary from 0.92 to 1.35. Sensitivity tests performed using these two end-member slope values show that the estimated, salinity-corrected $\delta^{18}O_{sw}$* at the LGM will only change by +0.02 to −0.03‰ compared to values obtained using a slope of 1.1.

[53] It is the small slope of the regional SSS-$\delta^{18}O_{sw}$ relationships that constitutes the weakest point of the whole correction procedure we propose here, since it may propagate large uncertainties. In order to test the sensitivity of our correction procedure to the regional SSS-$\delta^{18}O_{sw}$ relationship, we allowed the slope of the tropical Indian Ocean SSS-$\delta^{18}O_{sw}$ to change by plus 10% and minus 10% compared to its modern value (0.16). We applied then our correction procedure to LGM data from the warm-pool core MD98-2165 [*Levi*, 2003; *Waelbroeck et al.*, 2006; *Levi et al.*, 2007]. Allowing the modern SSS-$\delta^{18}O_{sw}$ slope to change by minus or plus 10% results in a shift of −0.37‰ and +0.35‰, respectively, on the estimated, LGM salinity-corrected $\delta^{18}O_{sw}$* of Core MD98-2165. This uncertainty propagates to the corrected temperature estimates, resulting on a ±1.7°C shift relative to estimates obtained using the modern slope.

[54] As we have just shown, the procedure developed to correct $\delta^{18}O_{sw}$ for the salinity bias on *G. ruber* Mg/Ca thermometry can carry on large uncertainties that cannot be easily quantified due to our incapacity to estimate true regional SSS-$\delta^{18}O_{sw}$ relationships over the past. Nevertheless, it is the authors' contention that our correction approach constitutes an improvement compared to estimate $\delta^{18}O_{sw}$ based on uncorrected $T_{Mg/Ca}$ values, which would potentially lead to large systematic errors. Same conclusion applies for temperatures. Due to the correction procedure, the salinity-corrected *G. ruber* temperature will carry on a large uncertainty, higher than the previously assumed uncertainty on Mg/Ca paleothermometry alone (∼1°C). However, choosing not to correct the salinity bias on Mg/Ca thermometry can lead to systematic errors (i.e., up to 1.6°C at the LGM if only the global salinity increase is considered).

6.5. Application of the Correction Procedure: Refining SST and $\delta^{18}O_{sw}$ Reconstructions in the Western Pacific Warm Pool Since the LGM

[55] We performed our correction procedure to estimate salinity-corrected SST and $\delta^{18}O_{sw}$* on one record from the Western Pacific Warm Pool that spans the time interval LGM-Holocene: Core

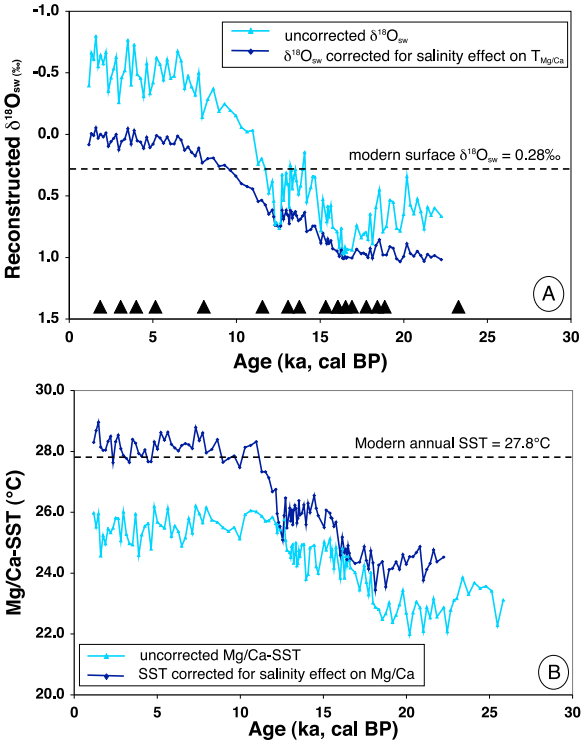

Figure 5. (a) Comparison of uncorrected $\delta^{18}O_{sw}$ and salinity-corrected $\delta^{18}O_{sw}$* of core MD98-2165 (Indonesian Archipelago region) plotted versus time (in cal Kyr BP). (b) Comparison of uncorrected $T_{Mg/Ca}$ and salinity-corrected SST of core MD98-2165 plotted versus time (in cal Kyr BP).

MD98-1265, recovered south of the Indonesian Archipelago during IMAGES cruise IV (9°38.96S, 118°20.31E, 2100 m water depth [*Levi*, 2003; *Waelbroeck et al.*, 2006; *Levi et al.*, 2007]). Global change in $\Delta\delta^{18}O_g$ (ice sheet effect) was derived from *Waelbroeck et al.* [2002]. Salinity-corrected $\delta^{18}O_{sw}$* and T_{iso} are compared with uncorrected $\delta^{18}O_{sw}$ and $T_{Mg/Ca}$ in Figure 5.

[56] As can be seen (Figure 5a), local effects of evaporation/precipitation result in an overall $\delta^{18}O_{sw}$* change between the LGM and the Holocene that is slightly smaller than the global ice volume effect (i.e., 1.05 ‰). This suggests that precipitation had increased (or evaporation decreased) at the LGM relative to the Holocene in the Warm Pool area at site of Core MD98-2165.

[57] The correction procedure introduces large changes in estimated SST compared to non-corrected estimates (Figure 5b). Not surprisingly, the recent Holocene values are much closer to the modern, atlas-derived data. As far as the LGM-Holocene change in SST is concerned, the amplitude is increased by +1.0°C when looking at the salinity-corrected SST compared to uncorrected $T_{Mg/Ca}$ (uncorrected LGM to Holocene SST change is ~3.0°C, whereas the salinity-corrected SST change is 4.0°C). It can be noted that the geometry of the SST record during the deglaciation is also affected by the correction procedure. The uncorrected SST record shows, for instance, a first major temperature increase at around 17.5 ka Cal BP, whereas the first major increase in the salinity-corrected SST is shifted around ~16 ka Cal BP. It is important to keep in mind, however, that over a glacial/interglacial transition, the correction procedure rests chiefly upon the correction (removal) of the global salinity effect on the *G. ruber* Mg/Ca SST. Like for any data processing that deals with substracting one record from another, small phasing inaccuracies may significantly alter the geometry of the salinity-corrected, Mg/Ca temperature record over the deglaciation, where rapid and large amplitude changes in global $\delta^{18}O_{sw}$ take place. Such phasing problems may be associated with uncertainties in the age model of the sediment core and/or the global $\delta^{18}O_{sw}$ reconstruction itself (i.e., *Lambeck and Chappell* [2001] give age uncertainties of up to ~1 kyr in their termination I sea level record). In addition, the relationship between sea level (salinity) and global ocean $\delta^{18}O$ signal is not linear during the deglaciation due to the reorganization of water masses, the propagation of the deglacial $\delta^{18}O$ signal and inhomogeneities in the ice sheet isotopic composition. Discussing thoroughly the deglaciation record of Core MD98-2165 is, therefore, beyond the scope of the present paper and will be the focus of another detailed study, which will compare various Mg/Ca records from the Western Pacific Warm Pool and other world ocean areas.

[58] There is still an ongoing debate about the SST cooling during the LGM compared to today in the tropical areas. The CLIMAP group, performing reconstructions using transfer function on planktonic foraminifera assemblages, concluded that the tropics only cooled by less than 2°C at the LGM, and possibly did not cool at all in some areas [*CLIMAP Project Members*, 1976]. More recently, the MARGO project (Multiproxy Approach for the Reconstruction of the Glacial Ocean surface) used modern statistical approaches and compiled several biogeochemical temperature proxies to reconstruct past oceanic temperatures. Although the revised SST changes in the tropical ocean since LGM have been increased compared to the CLIMAP results, it is still concluded that these changes were <3°C

[*Kucera et al.*, 2005; *MARGO Project Members*, 2009]. For instance, foraminiferal Mg/Ca indicated that the western tropical Pacific was 2.8 ± 0.7°C colder than the present at the Last Glacial Maximum [*Lea et al.*, 2000; *Rosenthal et al.*, 2003; *Visser et al.*, 2003]. Our results, however, indicate that the Western Pacific Warm Pool may have cooled by up to 4°C at the LGM compared to today when taking into account the salinity bias on Mg/Ca thermometry.

[59] Discrepancies between SST obtained from various proxies will need to be carefully addressed at a regional scale as they may result from a complex interplay of seasonality, surface water hydrographic structure and living depth of the different planktonic organisms. As far as the Western Pacific Warm Pool is concerned, for instance, *de Garidel-Thoron et al.* [2007] recently concluded that *G. ruber* Mg/Ca may have recorded the true sea surface temperature changes since the LGM, whereas planktonic foraminifera assemblages and Uk'_{37} thermometer have recorded subsurface temperature variations.

[60] A cooling of ~4°C in the tropics at the LGM appears to be in better accordance with the ~5°C cooling that was estimated based on Sr/Ca thermometry on corals [*Guilderson et al.*, 1994]. This stronger cooling of the tropical waters at the LGM appears to be also in better accordance with terrestrial evidences based on snow line reconstructions, vegetation changes [*Rind and Peteet*, 1985; *Broecker and Denton*, 1989], and noble gas dissolved in groundwater from various lowland tropical areas [*Stute et al.*, 1992, 1995; *Weyhenmeyer et al.*, 2000]. If confirmed by further studies, such a stronger cooling of the tropical oceans at LGM would have direct implications for our estimate of Earth's climate sensitivity to atmospheric pCO_2 [*Lea*, 2004; *Schneider von Deimling et al.*, 2006; *Hargreaves et al.*, 2007].

7. Conclusion

[61] We analyzed *G. ruber* specimens picked from 5 plankton tows retrieved in the West Pacific Ocean and 25 core tops located in the North Atlantic, the Red Sea, and the Indian and West Pacific tropical ocean in order to estimate the salinity effect on sea surface Mg/Ca temperature. The differences (ΔT) between Mg/Ca temperatures and calcification temperatures (measured in situ for plankton tows, and estimated from $\delta^{18}O$ measurements for core tops) correlate linearly with sea surface salinities. The positive slope of ~1.6, clearly indicates that salinity has a major effect on *G. ruber* Mg/Ca content (a +1 psu change in salinity leading to a +1.6°C bias in Mg/Ca temperature). Additional work is mandatory to check whether salinity of the ambient water also affects significantly the Mg/Ca of other planktonic species and its implications in past hydrographic reconstructions. We have developed a correction procedure to derive unbiased SST and $\delta^{18}O_{sw}$ from *G. ruber* $T_{Mg/Ca}$ and $\delta^{18}O_f$ measurements. This procedure applied to core MD98-2165 indicates a warming of the Western Pacific Warm Pool of ~4.0°C since the LGM; this is significantly higher than what was recently obtained in this area from uncorrected Mg/Ca thermometry [*Lea et al.*, 2000; *Rosenthal et al.*, 2003; *Visser et al.*, 2003].

Acknowledgments

[62] The authors thank J.-C. Duplessy, L. Labeyrie, E. Cortijo, E. Michel, M. Kageyama, and C. Waelbroeck for constructive discussions at various stages of this work. The authors also thank the two anonymous reviewers and a G-Cubed Associate Editor for their comments, which greatly improved the manuscript. This work was supported by French ANR as part of the FORCLIM project. It is LSCE contribution 4003.

References

Adkins, J. F., K. McIntyre, and D. P. Schrag (2002), The salinity, temperature and $\delta^{18}O$ of the glacial deep ocean, *Science*, *298*, 1769–1773, doi:10.1126/science.1076252.

Anand, P., H. Elderfield, and M. H. Conte (2003), Calibration of Mg/Ca thermometry in planktonic foraminifera from a sediment trap time series, *Paleoceanography*, *18*(2), 1050, doi:10.1029/2002PA000846.

Antonov, J. I., R. A. Locarnini, T. P. Boyer, A. V. Mishonov, and H. E. Garcia (2006), *World Ocean Atlas 2005*, vol. 2, *Salinity*, *NOAA Atlas NESDIS*, vol. 62, edited by S. Levitus, 182 pp., NOAA, Silver Spring, Md.

Arbuszewski, J., P. Demenocal, and A. Kaplan (2008), Towards a global calibration and validation of the G. ruber (white) Mg/Ca paleothermometer, *Eos Trans. AGU*, *89*(53), Fall Meet. Suppl., Abstract PP41F-02.

Archer, D. (1996), An atlas of the distribution of calcium carbonate in sediments of the deep sea, *Global Biogeochem. Cycles*, *10*, 158–159.

Bard, E., F. Rostek, and C. Sonzogni (1997), Interhemispheric synchrony of the last deglaciation inferred from alkenone palaeothermometry, *Nature*, *385*, 707–710, doi:10.1038/385707a0.

Barker, S., M. Greaves, and H. Elderfield (2003), A study of cleaning procedures used for foraminiferal Mg/Ca paleothermometry, *Geochem. Geophys. Geosyst.*, *4*(9), 8407, doi:10.1029/2003GC000559.

Bassinot, F. C., A. Baltzer, and the Shipboard Scientific Party (2002), IMAGES VII cruise report, *Rapp. Campagnes à la Mer, 01*, 435 pp., Inst. Fr. pour la Rech. et la Technol. Polaires, Plouzané, France.

Bassinot, F., F. Mélieres, M. Gehlen, C. Levi, and L. Labeyrie (2004), Crystallinity of foraminifer shells: A proxy to reconstruct past CO_3^{2-} changes, *Geochem. Geophys. Geosyst.*, *5*, Q08D10, doi:10.1029/2003GC000668.

Beck, J., J. Recy, F. Taylor, R. Edwards, and G. Cabioch (1997), Abrupt changes in early Holocene tropical sea surface temperature derived from coral records, *Nature*, *385*, 705–707, doi:10.1038/385705a0.

Beck, L., F. Bassinot, M. Gehlen, P. Trouslad, S. Pellegrino, and C. Levi (2002), Detection limit improvement for Mg in marine foraminiferal calcite by using helium induced X-ray emission, *Nucl. Instrum. Methods Phys. Res.*, *190*, 482–487, doi:10.1016/S0168-583X(01)01264-2.

Broecker, W. S., and E. Clark (1999), $CaCO_3$ size distribution: A paleocarbonate ion proxy?, *Paleoceanography*, *14*, 596–604, doi:10.1029/1999PA900016.

Broecker, W., and G. Denton (1989), The role of ocean-atmosphere reorganizations in glacial cycles, *Geochim. Cosmochim. Acta*, *53*, 2465–2501, doi:10.1016/0016-7037(89)90123-3.

Brown, S., and H. Elderfield (1996), Variations in Mg/Ca and Sr/Ca ratios of planktonic foraminifera caused by post-depositional dissolution: Evidence of shallow Mg-dependent dissolution, *Paleoceanography*, *11*, 543–552, doi:10.1029/96PA01491.

Chen, M., C. Huang, U. Pflaumann, C. Waelbroeck, and M. Kucera (2005), Estimating glacial western Pacific sea-surface temperature: Methodological overview and data compilation of surface sediment planktic foraminifer faunas, *Quat. Sci. Rev.*, *24*, 1049–1062, doi:10.1016/j.quascirev.2004.07.013.

Cléroux, C. (2007), Variabilité au cours des derniers 20 000 ans de l'hydrologie de l'Atlantique tropical Nord et de l'actvité du Gulf Stream à partir de la composition isotopique de l'oxygène et de la composition en éléments trace des foraminifères planctoniques profonds, Ph.D. thesis, 163 pp., Univ. Paris XI Orsay, Paris.

Cléroux, C., E. Cortijo, P. Anand, L. Labeyrie, F. Bassinot, N. Caillon, and J.-C. Duplessy (2008), Mg/Ca and Sr/Ca ratios in planktonic foraminifera: Proxies for upper water column temperature reconstruction, *Paleoceanography*, *23*, PA3214, doi:10.1029/2007PA001505.

CLIMAP Project Members (1976), The surface of the ice-age Earth, *Science*, *191*, 1131–1137.

Conan, S., and G. Brummer (2000), Fluxes of planktic foraminifera in response to monsoonal upwelling on the Somalia Basin margin, *Deep Sea Res., Part II*, *47*, 2207–2227.

Curry, W., D. Ostermann, M. Guptha, and V. Ittekkot (1992), Foraminiferal production and monsoonal upwelling in the Arabian Sea: Evidence from sediment traps, *Geol. Soc. Spec. Publ.*, *64*, 93–106, doi:10.1144/GSL.SP.1992.064.01.06.

de Garidel-Thoron, T., Y. Rosenthal, L. Beaufort, E. Bard, C. Sonzogni, and A. Mix (2007), A multiptoxy assessment of the western equatorial Pacific hydrography during the last 30 kyr, *Paleoceanography*, *22*, PA3204, doi:10.1029/2006PA001269.

Dekens, P. S., D. W. Lea, D. K. Pak, and H. J. Spero (2002), Core top calibration of Mg/Ca in tropical foraminifera: Refining paleotemperature estimation, *Geochem. Geophys. Geosyst.*, *3*(4), 1022, doi:10.1029/2001GC000200.

Delaygue, G., E. Bard, and C. Rollion (2001), Oxygen isotope/salinity relationship in the northern Indian Ocean, *J. Geophys. Res.*, *106*(C3), 4565–4574, doi:10.1029/1999JC000061.

de Villiers, S., M. Greaves, and H. Elderfield (2002), An intensity ratio calibration method for the accurate determination of Mg/Ca and Sr/Ca of marine carbonates by ICP-AES, *Geochem. Geophys. Geosyst.*, *3*(1), 1001, doi:10.1029/2001GC000169.

Duplessy, J. C., L. Labeyrie, A. Juillet-Leclerc, F. Maitre, J. Duprat, and M. Sarnthein (1991), Surface salinity reconstruction of the North Atlantic Ocean during the Last Glacial Maximum, *Oceanol. Acta*, *14*, 311–324.

Duplessy, J. C., L. Labeyrie, and C. Waelbroeck (2002), Constraints on the ocean oxygen isotopic enrichment between the Last Glacial Maximum and the Holocene: Paleoceanographic implications, *Quat. Sci. Rev.*, *21*, 315–330, doi:10.1016/S0277-3791(01)00107-X.

Elderfield, H., and G. Ganssen (2000), Past temperature and $\delta^{18}O$ of surface ocean waters inferred from foraminiferal Mg/Ca ratios, *Nature*, *405*, 441–445.

Elderfield, H., M. Vautravers, and M. Cooper (2002), The relationship between shell size and Mg/Ca, Sr/Ca, $\delta^{18}O$, and $\delta^{13}C$ of species of planktonic foraminifera, *Geochem. Geophys. Geosyst.*, *3*(8), 1052, doi:10.1029/2001GC000194.

Fairbanks, R. G. (1989), A 17000 year glacio-eustatic sea-level record: Influence of glacial melting rates on the Younger Dryas event and deepocean circulation, *Nature*, *342*, 637–642.

Ferguson, J., G. Henderson, M. Kucera, and R. Rickaby (2008), Systematic change of foraminiferal Mg/Ca ratios across a strong salinity gradient, *Earth Planet. Sci. Lett.*, *265*, 153–166, doi:10.1016/j.epsl.2007.10.011.

Guilderson, T., R. Fairbanks, and J. Rubenstone (1994), Tropical temperature variations since 20,000 years ago: Modulating interhemispheric climate change, *Science*, *263*, 663–665, doi:10.1126/science.263.5147.663.

Guilderson, T., R. Fairbanks, and J. Rubenstone (2001), Tropical Atlantic coral oxygen isotopes: Glacial-interglacial sea surface temperatures and climate change, *Mar. Geol.*, *172*, 75–89, doi:10.1016/S0025-3227(00)00115-8.

Hargreaves, J. C., A. Abe-Ouchi, and J. D. Annan (2007), Linking glacial and future climates thourgh ensemble of GCM simulations, *Clim. Past*, *2*, 77–87.

Kisakürek, B., A. Eisenhauer, F. Böhm, D. Garbe-Schönberg, and J. Erez (2008), Controls on shell Mg/Ca and Sr/Ca in cultured planktonic foraminiferan, *Globigerinoides ruber* (white), *Earth Planet. Sci. Lett.*, *273*, 260–269, doi:10.1016/j.epsl.2008.06.026.

Kucera, M., et al. (2005), Reconstruction of sea-surface temperatures from assemblages of planktonic foraminifera: Multi-technique approach based on geographically constrained calibration data sets and its application to glacial Atlantic and Pacific oceans, *Quat. Sci. Rev.*, *24*, 951–998, doi:10.1016/j.quascirev.2004.07.014.

Labeyrie, L. D., J. C. Duplessy, and P. L. Blanc (1987), Variations in mode of formation and temperature of oceanic deep waters over the past 125,000 years, *Nature*, *327*, 477–482, doi:10.1038/327477a0.

Lambeck, K., and J. Chappell (2001), Sea level change through the last glacial cycle, *Science*, *292*, 679–686, doi:10.1126/science.1059549.

Lea, D. (2004), The 100,000-yr cycle in tropical SST, greenhouse forcing and climate sensitivity, *J. Clim.*, *17*, 2170–2179, doi:10.1175/1520-0442(2004)017<2170:TYCITS>2.0.CO;2.

Lea, D., T. Mashiotta, and H. Spero (1999), Controls on magnesium and strontium uptake in planktonic foraminifera determined by live culturing, *Geochim. Cosmochim. Acta*, *63*, 2369–2379, doi:10.1016/S0016-7037(99)00197-0.

Lea, D. W., D. K. Pak, and H. J. Spero (2000), Climate impact of late quaternary equatorial Pacific sea surface temperature

variations, *Science*, *289*, 1719–1724, doi:10.1126/science.289.5485.1719.

LeGrande, A., and G. Schmidt (2006), Global gridded data set of the oxygen isotopic composition in seawater, *Geophys. Res. Lett.*, *33*, L12604, doi:10.1029/2006GL026011.

Levi, C. (2003), Etude des variations climatiques de la zone Indo-Pacifique: Rôle des basses latitudes dans la variabilité millénaire du climat, Ph.D. thesis, 181 pp., Univ. Paris XI Orsay, Paris.

Levi, C., L. Labeyrie, F. Bassinot, F. Guichard, E. Cortijo, C. Waelbroeck, N. Caillon, J. Duprat, T. de Garidel-Thoron, and H. Elderfield (2007), Low-latitude hydrological cycle and rapid climate changes during the last deglaciation, *Geochem. Geophys. Geosyst.*, *8*, Q05N12, doi:10.1029/2006GC001514.

Locarnini, R. A., A. V. Mishonov, J. I. Antonov, T. P. Boyer, and H. E. Garcia (2006), *World Ocean Atlas 2005*, vol. 1, *Temperature*, *NOAA Atlas NESDIS*, vol. 61, edited by S. Levitus, 182 pp., NOAA, Silver Spring, Md.

MARGO Project Members (2009), Constraints on the magnitude and patterns of ocean cooling at the Last Glacial Maximum, *Nat. Geosci.*, *2*, 127–132, doi:10.1038/ngeo411.

Mashiotta, T., D. Lea, and H. Spero (1999), Glacial-interglacial changes in Subantarctic sea surface temperature and δ^{18}O-water using foraminiferal Mg, *Earth Planet. Sci. Lett.*, *170*, 417–432, doi:10.1016/S0012-821X(99)00116-8.

Mathien-Blard, E. (2008), Révision du paléothermomètre Mg/Ca et son application sur l'hydrologie de surface de l'Océan Indien Tropical au cours de l'Holocène, Ph.D. thesis, 166 pp., Univ. Paris XI Orsay, Paris.

Nouet, J., and F. Bassinot (2007), Dissolution effects on the crystallography and Mg/Ca content of planktonic foraminifera *Globorotalia tumida* (Rotaliina) revealed by X-ray diffractometry, *Geochem. Geophys. Geosyst.*, *8*, Q10007, doi:10.1029/2007GC001647.

Nürnberg, D., J. Bijma, and C. Hemleben (1996), Assessing the reliability of magnesium in foraminiferal calcite as a proxy for water mass temperatures, *Geochim. Cosmochim. Acta*, *60*, 803–814, doi:10.1016/0016-7037(95)00446-7.

Oomori, T., H. Kaneshima, Y. Maezato, and Y. Kitano (1987), Distribution coefficient of Mg 2+ ions between calcite and solution at 10–50°C, *Mar. Chem.*, *20*, 327–336, doi:10.1016/0304-4203(87)90066-1.

Peeters, F., G. Brummer, and G. Ganssen (2002), The effect of upwelling on the distribution and stable isotope composition of *Globigerina bulloides* and *Globigerinoides ruber* (planktic foraminifera) in modern surface waters of the NW Arabian Sea, *Global Planet. Change*, *34*, 269–291, doi:10.1016/S0921-8181(02)00120-0.

Rashid, H., B. Flower, R. Poore, and T. Quinn (2007), A ~25 ka Indian Ocean monsoon variability record from the Andaman Sea, *Quat. Sci. Rev.*, *26*, 2586–2597, doi:10.1016/j.quascirev.2007.07.002.

Rind, D., and D. Peteet (1985), Terrestrial conditions at the last glacial maximum and CLIMAP sea-surface temperature estimates: Are they consistent?, *Quat. Res.*, *24*, 1–22, doi:10.1016/0033-5894(85)90080-8.

Rohling, E., and G. Bigg (1998), Paleosalinity and δ^{18}O: A critical assessment, *J. Geophys. Res.*, *103*(C1), 1307–1318, doi:10.1029/97JC01047.

Rosenthal, Y., and G. P. Lohmann (2002), Accurate estimation of sea surface temperatures using dissolution-corrected calibrations for Mg/Ca paleothermometry, *Paleoceanography*, *17*(3), 1044, doi:10.1029/2001PA000749.

Rosenthal, Y., D. W. Oppo, and B. K. Linsley (2003), The amplitude and phasing of climate change during the last deglaciation in the Sulu Sea, western equatorial Pacific, *Geophys. Res. Lett.*, *30*(8), 1428, doi:10.1029/2002GL016612.

Rosenthal, Y., et al. (2004), Interlaboratory comparison study of Mg/Ca and Sr/Ca measurements in planktonic foraminifera for paleoceanographic research, *Geochem. Geophys. Geosyst.*, *5*, Q04D09, doi:10.1029/2003GC000650.

Rostek, F., G. Ruhland, F. C. Bassinot, P. J. Muller, L. D. Labeyrie, Y. Lancelot, and E. Bard (1993), Reconstructing sea-surface temperature and salinity using δ^{18}O and alkenone records, *Nature*, *364*, 319–321, doi:10.1038/364319a0.

Russell, A., B. Hönisch, H. Spero, and D. Lea (2004), Effects of seawater carbonate ion concentration and temperature on shell U, Mg, and Sr in cultured planktonic foraminifera, *Geochim. Cosmochim. Acta*, *68*, 4347–4361, doi:10.1016/j.gca.2004.03.013.

Schneider von Deimling, T., H. Held, A. Ganopolski, and S. Rahmstorf (2006), Climate sensitivity estimated from ensemble simulations of glacial climate, *Clim. Dyn.*, *27*, 149–163, doi:10.1007/s00382-006-0126-8.

Sexton, P., P. Wilson, and P. Pearson (2006), Microstructural and geochemical perspectives on planktic foraminiferal preservation: "Glassy" versus "frosty," *Geochem. Geophys. Geosyst.*, *7*, Q12P19, doi:10.1029/2006GC001291.

Shackleton, N. J. (1974), Attainment of isotopic equilibrium between ocean water and benthonic foraminifera genus Uvigerina: Isotopic changes in the ocean during the last glacial, in *Les méthodes quantitatives d'étude des variations du climat au cours du Pleistocène*, pp. 203–209, Cent. Natl. de la Rech. Sci., Gif-sur Yvette, France.

Stute, M., P. Schlosser, J. F. Clark, and W. S. Broecker (1992), Paleotemperatures in the southwestern United States derived from noble gas measurements in groundwater, *Science*, *256*, 1000–1003, doi:10.1126/science.256.5059.1000.

Stute, M., M. Forster, H. Frischkorn, A. Serejo, J. F. Clark, P. Schlosser, and W. S. Broecker (1995), 5°C cooling of tropical Brazil during the last glacial maximum, *Science*, *269*, 379–383, doi:10.1126/science.269.5222.379.

Thompson, L., E. Mosley-Thompson, M. E. Davis, P. N. Lin, K. A. Henderson, J. Cole-Dai, J. F. Bolzan, and K. B. Liu (1995), Late glacial stage and Holocene tropical ice core records from Huascaran, Peru, *Science*, *269*, 46–50, doi:10.1126/science.269.5220.46.

Visser, K., R. Thunell, and L. Stott (2003), Magnitude and timing of temperature change in the Indo-Pacific warm pool during deglaciation, *Nature*, *421*, 152–155, doi:10.1038/nature01297.

Waelbroeck, C., L. Labeyrie, E. Michel, J. C. Duplessy, J. F. McManus, K. Lambeck, E. Balbon, and M. Labracherie (2002), Sea-level and deep water temperature changes derived from benthic foraminifera isotopic records, *Quat. Sci. Rev.*, *21*, 295–305, doi:10.1016/S0277-3791(01)00101-9.

Waelbroeck, C., C. Levi, J. C. Duplessy, L. Labeyrie, E. Michel, E. Cortijo, F. Bassinot, and F. Guichard (2006), Distant origin of circulation changes in the Indian Ocean during the last deglaciation, *Earth Planet. Sci. Lett.*, *243*, 244–251, doi:10.1016/j.epsl.2005.12.031.

Wang, L. (2000), Isotopic signals in two morphotypes of *Globigerinoides ruber* (white) from the South China Sea: Implications for monsoon climate change during the last glacial cycle, *Palaeoceanogr. Palaeoclimatol. Palaeoecol.*, *161*, 381–394, doi:10.1016/S0031-0182(00)00094-8.

Wang, L., M. Sarnthein, J. C. Duplessy, H. Erlenkeuser, S. Jung, and U. Pflaumann (1995), Paleo sea surface salinities in the low-latitude Atlantic: The δ^{18}O record of *Globigerinoides ruber* (white), *Paleoceanography*, *10*, 749–761, doi:10.1029/95PA00577.

Weyhenmeyer, C. E., S. J. Burns, H. N. Waber, W. Aeschbach-Hertig, R. Kipfer, H. H. Loosli, and A. Matter (2000), Cool glacial temperatures and changes in moisture source recorded in Oman groundwater, *Science*, *287*, 842–845, doi:10.1126/science.287.5454.842.

Zaric, S., B. Donner, G. Fischer, S. Mulitza, and G. Wefer (2005), Sensitivity of planktic foraminifera to sea surface temperature and export production as derived from sediment trap data, *Mar. Micropaleontol.*, *55*, 75–105, doi:10.1016/j.marmicro.2005.01.002.